

Provided for non-commercial research and education use.
Not for reproduction, distribution or commercial use.



This article appeared in a journal published by Elsevier. The attached copy is furnished to the author for internal non-commercial research and education use, including for instruction at the authors institution and sharing with colleagues.

Other uses, including reproduction and distribution, or selling or licensing copies, or posting to personal, institutional or third party websites are prohibited.

In most cases authors are permitted to post their version of the article (e.g. in Word or Tex form) to their personal website or institutional repository. Authors requiring further information regarding Elsevier's archiving and manuscript policies are encouraged to visit:

<http://www.elsevier.com/copyright>



Contents lists available at ScienceDirect

Journal of Biotechnology

journal homepage: www.elsevier.com/locate/jbiotec

Hydrogel-based protein and oligonucleotide microchips on metal-coated surfaces: Enhancement of fluorescence and optimization of immunoassay

Zh.I. Zubtsova*, D.A. Zubtsov, E.N. Savvateeva, A.A. Stomakhin, V.R. Chechetkin, A.S. Zasedatelev, A.Yu. Rubina

Engelhardt Institute of Molecular Biology of Russian Academy of Sciences, Vavilov str., 32, Moscow 119991, Russia

ARTICLE INFO

Article history:

Received 10 July 2009

Received in revised form 27 August 2009

Accepted 11 September 2009

Keywords:

Hydrogel-based protein and oligonucleotide microarrays
Metal-coated and glass substrates
Enhancement of fluorescence signal
Comparison of surface and gel-based microarrays
Quantitative immunoassay

ABSTRACT

Manufacturing of hydrogel-based microchips on metal-coated substrates significantly enhances fluorescent signals upon binding of labeled target molecules. This observation holds true for both oligonucleotide and protein microchips. When Cy5 is used as fluorophore, this enhancement is 8–10-fold in hemispherical gel elements and 4–5-fold in flattened gel pads, as compared with similar microchips manufactured on uncoated glass slides. The effect also depends on the hydrophobicity of metal-coated substrate and on the presence of a layer of liquid over the gel pads. The extent of enhancement is insensitive to the nature of formed complexes and immobilized probes and remains linear within a wide range of fluorescence intensities. Manufacturing of gel-based protein microarrays on metal-coated substrates improves their sensitivity using the same incubation time for immunoassay. Sandwich immunoassay using these microchips allows shortening the incubation time without loss of sensitivity. Unlike microchips with probes immobilized directly on a surface, for which the plasmon mechanism is considered responsible for metal-enhanced fluorescence, the enhancement effect observed using hydrogel-based microchips on metal-coated substrates might be explained within the framework of geometric optics.

© 2009 Elsevier B.V. All rights reserved.

1. Introduction

Matrix microchips with $M \times N$ arrays of elements containing immobilized probes (DNA, proteins, oligosaccharides, etc.) specific to various target molecules in analyte solution provide efficient tools for high-throughput analysis in different research and practical fields (Angenendt, 2005; Chechetkin et al., 2006; Chen and Zhu, 2006; Pollack, 2007; Rubina et al., 2008; Stoughton, 2005).

The immobilization of probes in individual elements may be performed either directly on a flat surface of glass, plastic, or metal substrate (Angenendt, 2005; Chen and Zhu, 2006; Pollack, 2007; Stoughton, 2005) or within gel pads attached to a substrate (Rubina et al., 2008). As has been shown earlier, the presence of nearby metallic surfaces or particles in the proximity of fluorophore molecules can dramatically affect the fluorescence intensity (for a recent review and further references see, e.g. Aslan et al., 2005; Lakowicz, 2005; Sabanayagam and Lakowicz, 2007; Sauer et al., 2005; Strohsahl et al., 2007). Depending on the distance between the fluorophore and metallic surface, as well as excitation conditions, the fluorescence intensity may either increase or decrease.

Previously, such an effect was demonstrated for two-dimensional (surface) microchips on metal-coated slides and for probes immobilized on nanoparticles. On both platforms, enhanced fluorescence intensity and improved sensitivity were achieved (Aslan et al., 2005; Lakowicz, 2005; Sabanayagam and Lakowicz, 2007; Sauer et al., 2005; Strohsahl et al., 2007).

This paper presents the study of fluorescence enhancement on hydrogel-based oligonucleotide and protein microchips manufactured on metal-coated substrates. Using Cy3- and Cy5-labeled probe and target molecules, we demonstrate that the coating increases fluorescence intensity 8–10-fold on microchips with hemispherical gel pads and 4–5-fold on microchips with flattened pads as compared with microchips on glass substrates without coating. Metal-enhanced fluorescence on hydrogel-based microchips depends on the shape of gel pads and on the presence of liquid over gel pads. To assess the applicability of enhancement effect, we investigated the sensitivity of metal-enhanced fluorescence to the type of formed molecular complexes (from mono to quadruple) and the range of linear dependence of fluorescence signals on concentration of labeled molecules. The enhancement of fluorescence for microchips on metal-coated substrates allows improving sensitivity of immunoassay and/or significant shortening of the time of analysis.

Our results indicate that, unlike surface microchips, the main features of enhancement effect on hydrogel-based microchips with

* Corresponding author. Fax: +7 495 135 14 05.

E-mail address: zubtsova.z.i@gmail.com (Zh.I. Zubtsova).

metal-coated substrates may be explained within the concepts of geometric optics.

2. Materials and methods

2.1. Chemicals and analytes

Chemical reagents obtained from commercial suppliers were used without further purification. Purified prostate specific antigen (PSA) was purchased from Khema-Medica (Moscow, Russia). Concentrations of PSA in solution for PSA_{free} and PSA_{total} were determined using Fujirebio Diagnostics enzyme immunoassay kits from CanAg (Sweden). Monoclonal antibodies against PSA were also from CanAg. We used immobilized monoclonal antibodies PSA36 and developing antibodies PSA66, both recognizing PSA. Cholera anatoxin (Sigma, St. Louis, USA) and monoclonal antibodies CHG9 and CHT3D6 to cholera anatoxin were kindly provided by Prof. V.A. Nesmejanov from the Institute of Bioorganic Chemistry (Moscow, Russia). Bovine serum albumin (BSA), 2-methyl-4-isothiazolin-3-one hydrochloride (MIT), polyvinyl alcohol (PVA), 50 kDa, polyvinyl pyrrolidone (PVP), 360 kDa, N-hydroxysuccinimidobiotin, Sephadex G-25 coarse, and Tween-20 were obtained from Sigma (St. Louis, USA); Cy5 fluorescence dye, Cy3 fluorescence dye monosuccinimide ester, Cy5-labeled streptavidin and Bind Silane from Amersham Pharmacia Biosciences (Pittsburgh, PA, USA); and Micro Bio-Spin chromatography columns from Bio-Rad Laboratories (Hercules, CA, USA); Glycerol was obtained from Sigma (St. Louis, USA). Transparent plastic chambers 25 μ l in volume (area 1 cm \times 1 cm, height 250 μ m) from Eppendorf Scientific (Germany) and custom-made chambers 60 μ l in volume (area 0.8 cm \times 1.2 cm, height 600 μ m) were used for on-chip-analysis. The oligonucleotide probes 5'-AAATAT-3' containing 5'-terminal amino groups and 3'-terminal Cy5-dyes were synthesized using a 394 DNA/RNA synthesizer (Applied Biosystems, Foster City, CA, USA) by standard phosphoramidite chemistry from Glen Research (Sterling, VA, USA). Oligonucleotides were purified by reverse-phase HPLC on a Supelco LC-18 column (5 μ m, 4.6 mm \times 250 mm) using 0.05 M triethylammonium acetate, pH 7.0, with gradient of CH₃CN from 0 to 50%. We used the following buffers: PBS (0.01 M phosphate buffer, pH 7.2, 0.15 M NaCl); PBST (PBS with 0.1% Tween-20); blocking solution PBSP (PBS with 1% polyvinyl alcohol); buffer for antibody dilution MIX1 (PBS with 0.14% polyvinyl alcohol, 0.14% polyvinyl pyrrolidone, and 10 mg/ml BSA); and buffer for antigen dilution MIX2 (MIX1 with 0.1% Tween-20). Gel pads synthesized on microchips were visualized using Leica TCS confocal microscope (Germany) with laser excitation wavelength 548 nm. The images were processed using Leica software.

2.2. Substrates for microchips

Glass slides for the fabrication of microarrays (Corning 2947 Micro Slides; 3 in. \times 1 in.) were from Corning Glass Works (Corning, NY, USA). The slides were treated with NaOH, H₂SO₄, rinsed with water, then immersed in 1% Bind Silane in ethyl alcohol, treated with ethyl alcohol, rinsed with water, and dried. Gold-coated slides 25 mm \times 75 mm (Nunc 231644 Microarray slides with 120 nm gold film coating) from Nunc A/S (Nunc, Roskilde, Denmark) were used without additional treatment. We also used glass slides coated with nickel, chromium, or aluminum (Mikron, Zelenograd, Russia). To manufacture these, Corning glass slides were first coated with 80 nm thick layer of titanium using electron beam evaporation; then a 250 nm layer of nickel, chromium, or aluminum was added.

2.3. Fabrication of microchips

Gel-based microchips were fabricated by copolymerization immobilization method developed earlier (Mirzabekov et al., 2003; Rubina et al., 2003, 2004, 2005). Solutions containing gel-forming monomers methacrylamide and N-substituted amino sugars together with immobilized proteins or oligonucleotides were spotted onto substrates using a QArray pin robot (Genetix, New Milton, UK). The volume of spotting solution was about 0.1 nl per spot. The distance between the centers of gel elements was 250 μ m. To increase the accuracy of the measurements, each set corresponding to a given concentration of probes in spotting solution consisted of four gel pads. Polymerization of the gel-forming composition was carried out under UV light with maximal wavelength 350 nm, irradiation intensity 0.06 μ W/cm² (GTE lamp F15T8/350 BL, Sylvania, Danvers, MA), for 50 min at 20 °C in nitrogen flow.

2.4. Labeling with Cy3 and Cy5 fluorescence dyes

Monoclonal antibodies were labeled at amino groups with either Cy5 or Cy3 succinimide ester according to the manufacturer's instructions. The excess of the dye was removed by gel filtration on a Micro Bio-Spin column with Sephadex G-25 coarse. The protein:dye molar ratio was determined by the absorbance at 280 and 550 or 650 nm for Cy3 or Cy5, correspondingly.

2.5. Preparation of antibody-biotin conjugates

Ten microliters of N-hydroxysuccinimidobiotin (5 mg/ml in dimethyl formamide) were added to 70 μ l antibody solution (5 mg/ml in 0.01 M bicarbonate buffer, pH 9.8), and the mixture was stirred for 1 h at 20 °C. Antibody-biotin conjugates were purified on a Micro Bio-Spin column with Sephadex G-25 coarse equilibrated with PBS.

2.6. Immunoassay

Gel-based antibody microchips were prepared for immunoassay by printing on either uncoated or metal-coated glass slides. Before carrying out on-chip immunoassays, microchips with antibodies were treated with PBST for 40 min and rinsed with water. For suppression of non-specific binding, the microchips were treated with blocking buffer PBSP for 1 h and then rinsed with water.

2.7. One-stage sandwich immunoassay for PSA

Microchips for PSA immunoassay consisted of gel pads with 0.7 mg/ml of immobilized antibodies PSA36. Ten microliters of developing Cy5-labeled antibodies PSA66 in MIX2 (concentration 3.5 μ g/ml) were added to 50 μ l of PSA in MIX1. The mixture was stirred carefully and applied on the biochips using a pipette through one of the outlets of the reaction chamber. The reaction chambers were sealed with tape and microchips were incubated for 20 h at 37 °C. After incubation, reaction chambers were removed from the microchips, and the microchips were rinsed with water, washed with PBST buffer for 30 min at room temperature on a shaker, again rinsed with water, dried in the air, and used for fluorescent measurements.

2.8. Sandwich immunoassay for cholera anatoxin using avidin-biotin complex

Gel pads of microchips for cholera anatoxin immunoassay contained 1.5 mg/ml of immobilized antibodies CHG9. For on-chip immunoassay, 30 μ l of developing antibody conjugate

CHT3D6–biotin in MIX1 (concentration 20 µg/ml) were added to 30 µl of cholera anatoxin in MIX1. The mixture was stirred and applied on microchips. The microchips on uncoated glass slides were incubated for 20 h at 37 °C, while for the microchips on metal-coated substrates the incubation time was 2 h. After incubation, microchips were rinsed with water, washed with PBST buffer for 20 min at room temperature on a shaker, again rinsed with water, and air-dried. Then, 50 µl of Cy5-labeled streptavidin in MIX1 (concentration 10 µg/ml) was applied on the microchips and incubated for 1 h at room temperature. After incubation, the microchips were rinsed with water, washed with PBST for 30 min at room temperature on a shaker, again rinsed with water, air-dried, and used for fluorescent measurements.

2.9. Measurements of fluorescence signals

Quantitative fluorescence measurements were carried out with an analyzer (Biochip-EIMB, Russia) consisting of a fluorescence microscope, cooled CCD camera, and a computer with data-acquisition board (Barsky et al., 2002). The scheme of fluorescent microscope is shown in Fig. 1 (panel A). The four lasers emitted the excitation radiation incident at the angle 45° with respect to the plane of microchip. The fluorescence radiation from microchip gone through the objective with videoadapter, then through the filter and received by CCD camera. The filter cut off the light reflected from the surface of microchip (note that the wavelength of excitation light is shorter than the wavelength of fluorescence radiation due to Stokes rule). The data from CCD camera were sent to computer and processed by the program ImaGel. The signals from Cy5 dye were obtained using 649/670 nm excitation/emission filters, whereas the signals from Cy3 dye were obtained using 549/570 nm excitation/emission filters. The exposure time for cholera anatoxin immunoassay was 1000 ms, in all other cases –200 ms. All measurements were carried out at room temperature. Fluorescence signals from individual pads were processed using ImaGel Research program (IMB, Russia). Fluorescence intensity of individual elements was calculated by the formula

$$J = \frac{C - B_{d.c.}}{B_{r.g.} - B_{d.c.}} \quad (1)$$

where C is the median fluorescence calculated for the image area occupied by the element (i.e. median value for the set of pixels covering image area). To take into account possible spatial inhomogeneity of radiation from illumination source, the microchip was replaced with a slide of identical size made of red glass, and the corresponding median fluorescence intensity within the area occupied by the gel pad, $B_{r.g.}$, was measured. The values of signals C and $B_{r.g.}$ were corrected by noise signal $B_{d.c.}$ produced by dark current at zero illumination intensity. Since the dependence of fluorescence signal on the intensity of excitation light is linear, the ratio (1) is insensitive to the variations of illumination.

3. Results

In our work we used microchips with three-dimensional hydrogel pads produced via technology based on the photoinduced polymerization immobilization of molecular probes simultaneously with the formation of gel pads on a microchip (Mirzabekov et al., 2003; Rubina et al., 2003, 2004, 2005). For the experiments on the assessment of fluorescence enhancement, several sets of biochips were prepared. Microdrops of the solution containing gel-forming monomers and molecular probes were printed on either transparent or mirror-like metal-coated glass substrates. All experiments described in this work were repeated thrice. The relative scattering in experimental data did not exceed 15%. The data correspond to the median values for four-element sets with identical

Table 1

Enhancement of fluorescence on hydrogel-based microchips printed on substrates coated with different metals.

Substrate	Reflection coefficient		Signal enhancement	
	$\lambda = 550$ nm	$\lambda = 650$ nm	Cy3	Cy5
Glass	0.04	0.05	1.0	1.0
Glass coated with nickel	0.61	0.66	2.1 ± 0.1	2.1 ± 0.1
Glass coated with chromium	0.65	0.64	2.1 ± 0.1	2.0 ± 0.1
Glass coated with aluminum	0.91	0.91	4.5 ± 0.2	4.5 ± 0.3
Glass coated with gold	0.90	0.95	4.8 ± 0.2	4.5 ± 0.5

concentration of immobilized proteins or oligonucleotides (see Section 2 and Fig. 1, panel B).

It has to be stressed that metal-coated substrates significantly improve the signal-to-background ratio, which defines the sensitivity of signal detection. Background signal refers to the fluorescence intensity of the substrate itself. Comparison of fluorescent signals from gel elements manufactured on different types of substrates was achieved by selection of proper filter capable of cutting off the light from laser source reflected by the substrate and by adjusting the aperture of the sensor device. Thus, we were able to avoid artifacts caused by the reflection of excitation light from metallic surface.

This restriction is essential, because in principle the intensity of signals from the pads might be increased by longer exposure time. In this case, however, the longer exposure time would also result in the increase of background signals, whereas signal-to-background ratio would remain constant regardless of the exposure time.

3.1. General factors affecting metal-enhanced fluorescence on gel-based microchips

3.1.1. Enhancement of fluorescence on hydrogel biochips manufactured on metal-coated substrates: comparison of fluorophores and metals

In the course of our study of the enhancement of fluorescence on hydrogel microchips, we tested coating with four metals (nickel, chromium, aluminum, and gold) and two fluorophores, Cy3 and Cy5. The enhancement of fluorescence was observed for both fluorophores as well as for all metals used for coating, and the data for all combinations are compiled in Table 1 (where the data on reflection coefficients were taken from the book by Weaver et al., 1981). They clearly indicate that the level of enhancement directly correlates with the reflective ability of the substrate. The nature of fluorescence enhancement is of physical origin and is insensitive to the type of complexes formed in the gel pads with immobilized probes (see also below). The combination of gold coating and Cy5 fluorophore was chosen for more detailed investigation.

3.1.2. Enhancement of fluorescence intensity and its dependence on the shape of gel pads

The relative enhancement of fluorescence intensity for gel-based microchips manufactured on metal-coated and glass substrates is shown in Fig. 2. All data refer to semi-dry microchips analyzed without buffer solution. As is seen from Fig. 2, the metal coating provides 4–5-fold increase in fluorescence signals as compared with identical gel elements on plain surface. This increase is observed after washing and drying of the microchips and does not depend on the nature of complexes or labeled immobilized compounds. Such an enhancement of the fluorescence attains 8–10-fold level if the microchips are left unwashed or are treated after drying with glycerol solution for re-hydration.

We hypothesized that one of the factors affecting such a difference in fluorescence enhancement may be the change in the shape of gel elements upon dehydration (see Fig. 3A and B). The

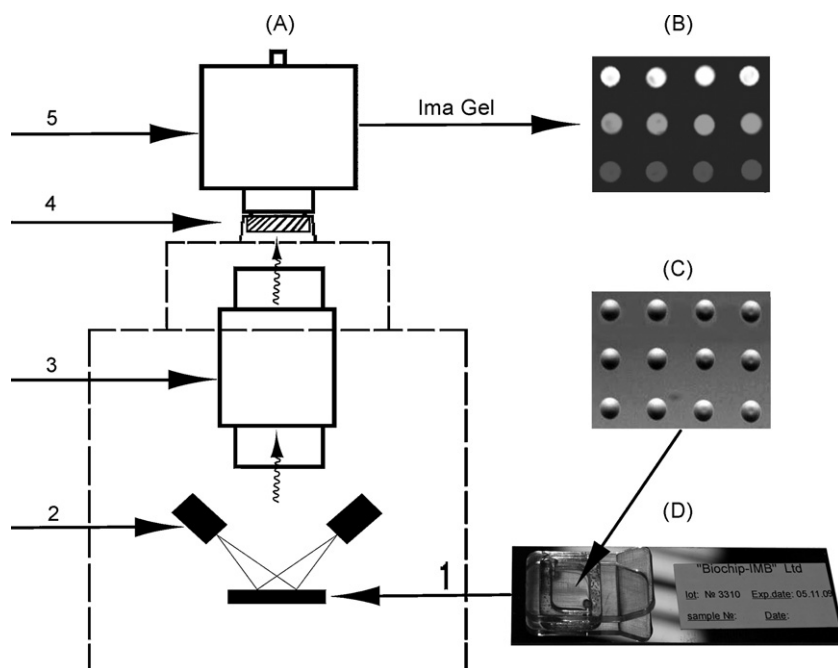


Fig. 1. The general scheme of analyzer used in our experiments. (A) Fluorescent microscope. The excitation radiation from four lasers (2) induced the fluorescence on microchip (1). The fluorescence radiation from microchip gone through the objective with videoadapter (3), then through the filter (4) cut off the excitation light reflected from the microchip surface and received by CCD camera (5). The data from CCD camera were sent to computer and processed by the program ImaGel (panel B). The microchip and the gel pads in the transmitted light are shown in panels D and C, respectively. The concentration of antibodies immobilized in all four pads in each row was identical (panel B).

unwashed gel pads after printing contain glycerol, are hydrated, and their shape is close to hemispherical. The height of gel elements on glass and gold-coated substrates was $50 \pm 3 \mu\text{m}$ and the radii of elements were $60 \pm 2 \mu\text{m}$. After washing out glycerol, the gel pad dries within a few minutes and becomes much more flat. It is worth noting that, although the height of gel elements after drying diminishes, the shape of identical pads on glass and metal-coated substrates remains essentially similar. For example, the height and the radii of gel elements on both glass and metal-coated substrates after washing and drying were $25 \pm 3 \mu\text{m}$ and $60 \pm 2 \mu\text{m}$, respectively.

We also compared the relative enhancement of fluorescence signals for slides covered with $30 \mu\text{m}$ thick layer of gel containing Cy5-labeled BSA at the same concentration as Cy5-labeled BSA immobilized in the gel pads. The layer occupied a rectangle $0.8 \text{ cm} \times 1.2 \text{ cm}$. After washing and drying, we observed 4-fold enhancement of fluorescence on metal-coated surface as compared with plain glass substrate, similar to the enhancement observed on dried gel pads. Taking into account the flattened form of dried pads (see Fig. 3B), such a correspondence seems reasonable.

The shape of re-hydrated gel pads under a layer of liquid resembles their shape after printing and polymerization (see Fig. 3A and C). The addition of 50% glycerol solution in water to dried microchips results in the swelling of gel pads to hemispherical form as shown by confocal microscopy (cf. Fig. 3A). Subsequent removal of the excess of glycerol solution in air flow restores 8-fold enhancement of fluorescence (columns 1a and 2a in Fig. 2B) as compared with similar pads on glass surface. After re-hydration of flattened gel pads with glycerol solution, the fluorescence signals from the gel pads on glass increase about 1.5-fold, whereas those from the pads on metal-coated substrates increase about thrice.

3.1.3. Fluorescence enhancement under a layer of liquid

Fig. 4 illustrates the effects of water covering the microchip with gel-immobilized Cy5-labeled BSA on fluorescence signals. The measurements were carried out in plastic chambers $25 \mu\text{l}$ in volume.

These results demonstrate that the presence of a layer of water suppresses the relative fluorescence enhancement from ~ 8 – 10 -fold in hydrated gel pads and ~ 4 – 5 in partially dried gel pads to ~ 2 – 3 on microchips submerged in water, despite the preservation of the hemispherical form of the gel pads. After removal of the chamber and drying of liquid covering the microchip, the shape of gel elements changes from swollen hemispherical form, when the enhancement of fluorescence is the highest, to flattened form, when the enhancement of fluorescence decreases to 4–5-fold (see Fig. 5).

3.1.4. Effects of optical coherence from illumination source on fluorescence enhancement

To exclude possible optical coherence effects from an illumination source on the metal-enhanced fluorescence from the pads on metal-coated substrate, we compared the level of enhancement using microchip analyzers with different light sources. We tested an analyzer with four excitation lasers (wavelength 655 nm, incidence angle $\sim 45^\circ$); an analyzer with two excitation lasers equipped with optical fiber for light transmission (wavelength 655 nm, incidence angle $\sim 45^\circ$); and an analyzer with mercury lamp as the light source (filtered excitation wavelength 650 nm, incidence angle $\sim 90^\circ$). In all three cases, the enhancement of fluorescence was similar: 4.3 ± 0.4 ; 4.0 ± 0.5 ; and 4.1 ± 0.4 .

3.1.5. Dependence of fluorescence signals and enhancement effect on concentration of immobilized probes

To assess possible non-linear dependence of fluorescence signals and metal-enhancement effect on the concentration of immobilized probes, we used microchips with Cy5-labeled BSA and 5'-AAATAT-3' immobilized at different concentrations. These data are shown in Fig. 6. The concentration dependence of signals for gel-based microchips is linear with a good accuracy and precision, whereas metal-enhancement effect remains insensitive to variations in concentration. It has to be noted that this dependence holds

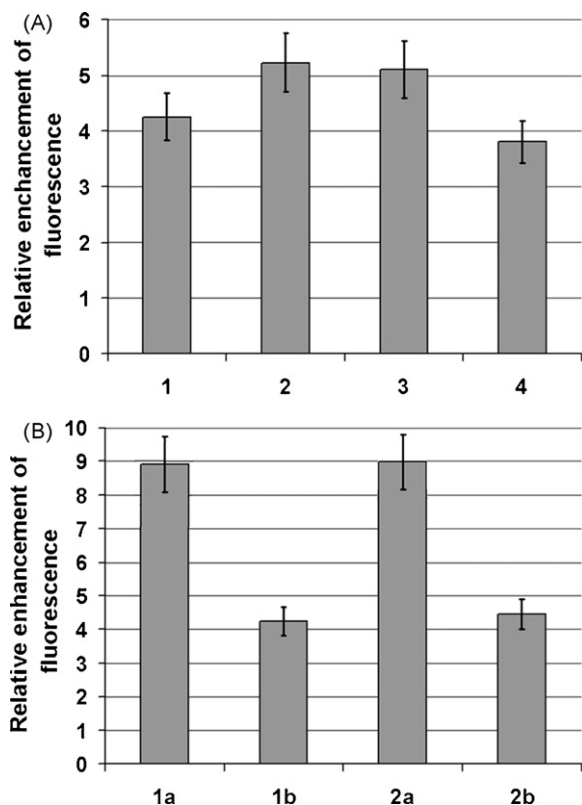


Fig. 2. Enhancement of fluorescence signals of gel-based microchips manufactured on metal-coated substrates. (A) 1, Immobilized Cy5-labeled bovine serum albumin (BSA); 2, Binary complexes between immobilized prostate specific antigen (PSA) and Cy5-labeled antibodies; 3, Sandwich immunoassay for PSA (triple complexes of immobilized antibody, antigen, and developing antibody); and 4, Immunoassay analysis for cholera anatoxins (quadruple complexes of immobilized antibody, anatoxin, biotinylated antibody, and Cy5-streptavidin-Cy5). Data in (A) refer to washed and dried microchips. (B) 1, Immobilized Cy5-labeled bovine serum albumin (BSA) before (a) and after (b) washing and drying; and 2, Immobilized Cy5-labeled oligonucleotides 5'-AAATAT-3' before (a) and after (b) washing and drying.

true also for the lowest detectable fluorescence intensities, which determine the sensitivity of immunoassays (see below).

The distance between the probe molecules inside the gel pads becomes comparable with their molecular size at concentrations $\sim 10^{-4}$ to 10^{-3} M. In our conditions, the highest concentrations remained two to three orders of magnitude lower than these values and corresponded to intermolecular distances of ~ 100 nm. This prevents potential interactions between the probe molecules. In our experiments we observed linear relation between the concentration of fluorophore and fluorescence intensity. Such dependence ensures independence of fluorescence enhancement on concentration.

3.2. Optimization of sandwich immunoassay

To demonstrate the practical advantages of protein microchips on metal-coated substrates for sandwich immunoassay, we used PSA, serum marker of prostate cancer (see *Konovalova et al., 2007* and references therein), and cholera anatoxin (inactivated analogue of natural biotoxin) immunoassays as examples. The efficiency of on-chip immunoassay was assessed by two parameters: enhancement of sensitivity and/or shortening of the time of analysis. For oncomarkers, the first parameter is particularly important, while in the case of biotoxins their rapid detection is of primary interest.

For PSA immunoassay, the same incubation times were used for microchips on metal-coated and uncoated glass slides. To assess the effect of fluorescence enhancement on the sensitivity of analy-

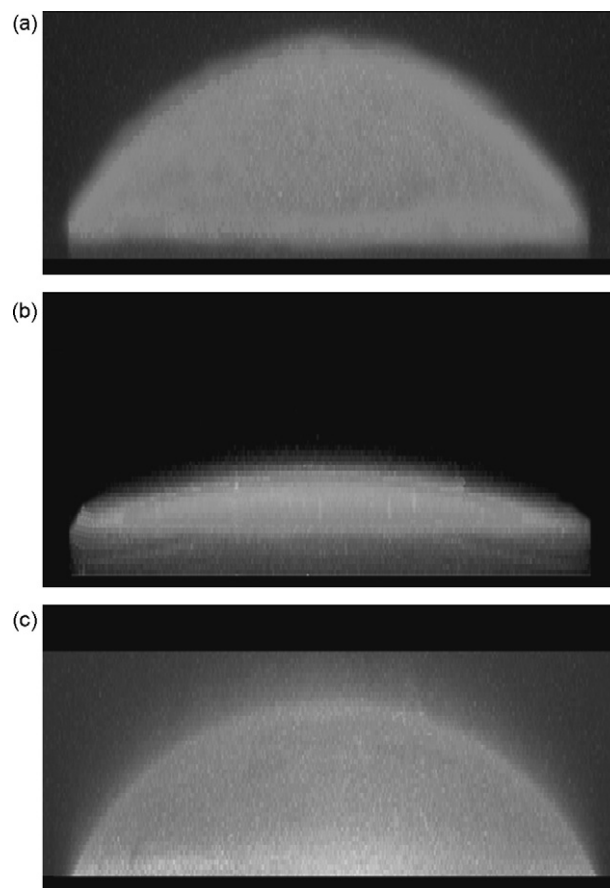


Fig. 3. Side view images of gel pads on the microchips on glass slides. (A) Hydrated gel pad (characteristic height ~ 50 μm); (B) Washed and then partially dried gel pad (height ~ 25 μm); and (C) Re-hydrated gel pad under the layer of liquid (height ~ 45 μm). All images were obtained with confocal microscope. The radii of the pads are 60 μm .

sis, the calibration curves for sandwich immunoassay of PSA were obtained using microchips printed on metal-coated and glass substrates. The concentration of antigen in solution was determined using calibration curves—plots of fluorescence intensity versus known control concentrations of antigen. The sensitivity of PSA immunoassay was determined as concentration corresponding to the level of fluorescence exceeding more than two standard devi-

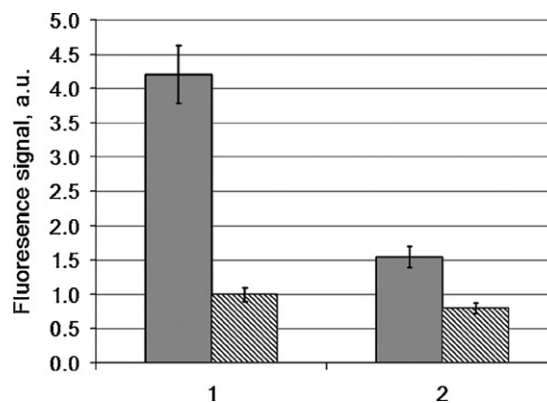


Fig. 4. Effect of liquid covering gel-based microchip with immobilized Cy5-labeled BSA on fluorescence signals. (1) Dried microchips without buffer solution; (2) Microchips under water in the chamber 250 μm in height. For each pair the left column corresponds to signals on metal-coated substrates, while the right column corresponds to that on plain glass substrates.

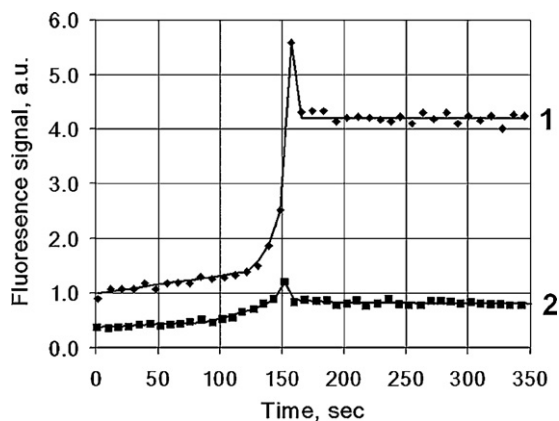


Fig. 5. Dynamics of fluorescence signals for wet gel-based microchips with immobilized Cy5-labeled bovine serum albumin during drying. (1) Metal-coated substrates; (2) Glass substrates. The peak of fluorescence signal at ~150 s corresponds to hydrated hemispherical gel pads immediately after evaporation of liquid layer. Afterwards, the gel pads dry rapidly and become flattened.

ations. Standard deviation was calculated by repetitive (more than 10 times) measurement of signals from control gel elements with zero concentration of antigen in the samples (Davis, 2005). As seen in Fig. 7A, with identical conditions of the reaction and incubation time, we obtained 4–5-fold enhancement of fluorescence signals for PSA calibration curve on metal-coated surfaces within the full range of concentrations. The sensitivity of PSA analysis increased from 0.2 ng/ml for microchips on transparent substrates to 0.05 ng/ml for microchips on metal-coated substrates. The corresponding kinetic curves for direct PSA analysis are presented in Fig. 7B (unlike Fig. 7A the relevant signals were measured under buffer solution).

As has been proved earlier, the developed multi-parametric test-system for the parallel quantitative analysis of oncomarkers set (PSA, alpha-fetoprotein, carcinoembryogenic antigen, CA-125, CA 19-9, CA 15-3, chorionic gonadotropin, and neuron-specific enolase) on the antibody microchips satisfies all the claims for immunoassay systems concerning the analytical characteristics, sensitivity, reproducibility, etc. (the detailed comparison may be found in Table 1 in the review by Rubina et al., 2008). These earlier data have been obtained for the microchips on glass substrates. Using microchips on metal-coated substrates allows one to enhance the sensitivity 4–5 times at the equal incubation times, as was shown for PSA in this work. The similar enhancement should be expected for the other oncomarkers as well in view of the physical nature and universality of enhancement effect.

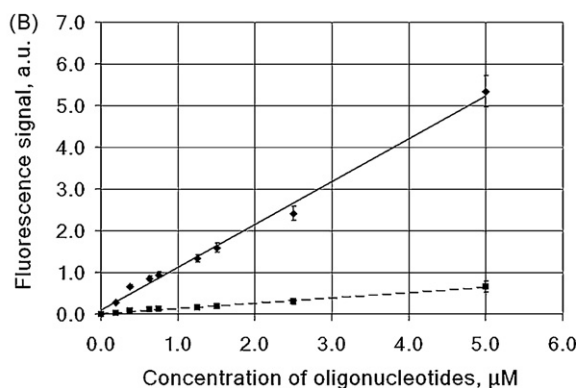
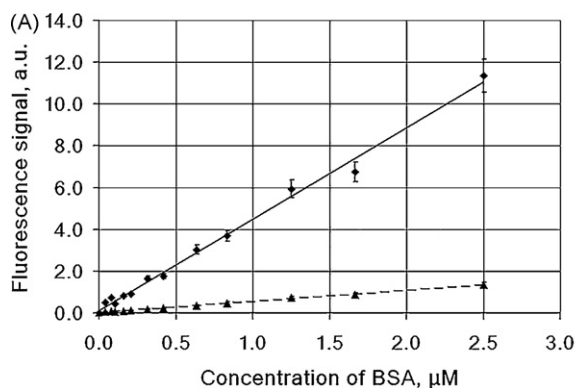


Fig. 6. Dependence of fluorescence signals for Cy5-labeled bovine serum albumin (A) and oligonucleotides 5'-AAATAT-3' (B) immobilized within gel pads on concentration of Cy5-labeled molecules in spotting solution. Solid lines correspond to Cy5-labeled molecules immobilized within gel pads on metal-coated substrates, while dashed lines correspond to that on glass substrates. The ratio of dye per probe molecule was about four for BSA-Cy5 and about one for oligonucleotide-Cy5. All data refer to the microchips without washing after printing.

Another way to take advantage of the enhancement effect in on-chip immunoassays is to shorten the time of analysis. For the analysis of cholera anatoxin we used sandwich immunoassay with avidin–biotin system for development. The mixture containing the anatoxin and developing biotinylated antibodies against this antigen was placed on the microchip with immobilized antibodies against cholera anatoxin. After completion of incubation and washing, the microchip was treated with fluorescently labeled streptavidin. In this protocol, the time-limiting stage is the formation of ternary complexes consisting of immobilized antibody, antigen, and biotinylated antibody. Earlier, we determined that 17 h of incubation was optimal for microchips prepared on glass substrate to reach the necessary signal intensity and sufficient sensitivity (Rubina et al., 2005). Here we demonstrate that the same level of signals and therefore sensitivity (5 ng/ml) can be attained after just 2 h of incubation with developing antibodies on microchips with metal-coated surface (Fig. 7B). The shortening of incubation time was made possible due to both metal-enhanced fluorescence and non-linearity of binding curves (see also Appendix A for discussion of kinetic effects on sensitivity). Thus, the application of protein microchips on metal-coated substrates with enhanced signal-to-background ratio can improve significantly two key characteristics of on-chip immunoassay: the sensitivity and the time of analysis.

4. Discussion

The interaction between a light-emitting fluorophore and nearby metal surface may be described in terms of fluorophore interactions with lossy surface waves, plasmon excitations, and reflected photons (Ford and Weber, 1984; Lakowicz, 2005). The interactions with plasmons and lossy surface waves are thought to be significant only at the distances less or about equal to the wavelength of excitation light (cf. Fig. 6 in paper by Lakowicz, 2005). Note that the optical properties the gel pads make them similar to dielectric cover of metal surface needed for efficient excitation of plasmons (Lakowicz, 2005). Since the excitation wavelength for Cy5 is 650 nm, whereas the heights of dehydrated flattened and hydrated hemispherical gel pads are about 25 and 50 μm, respectively, the interactions of a fluorophore with plasmons and lossy surface waves are restricted to a thin layer in the immediate proximity to metal surface. Therefore, even if the plasmon mechanism contributes to observable fluorescence enhancement, its role for gel-based microchips cannot be as significant as for surface microchips.

Optically, a gel pad on metal surface may act as a convex collecting lens (Born and Wolf, 1980). It is also known that the spectrum

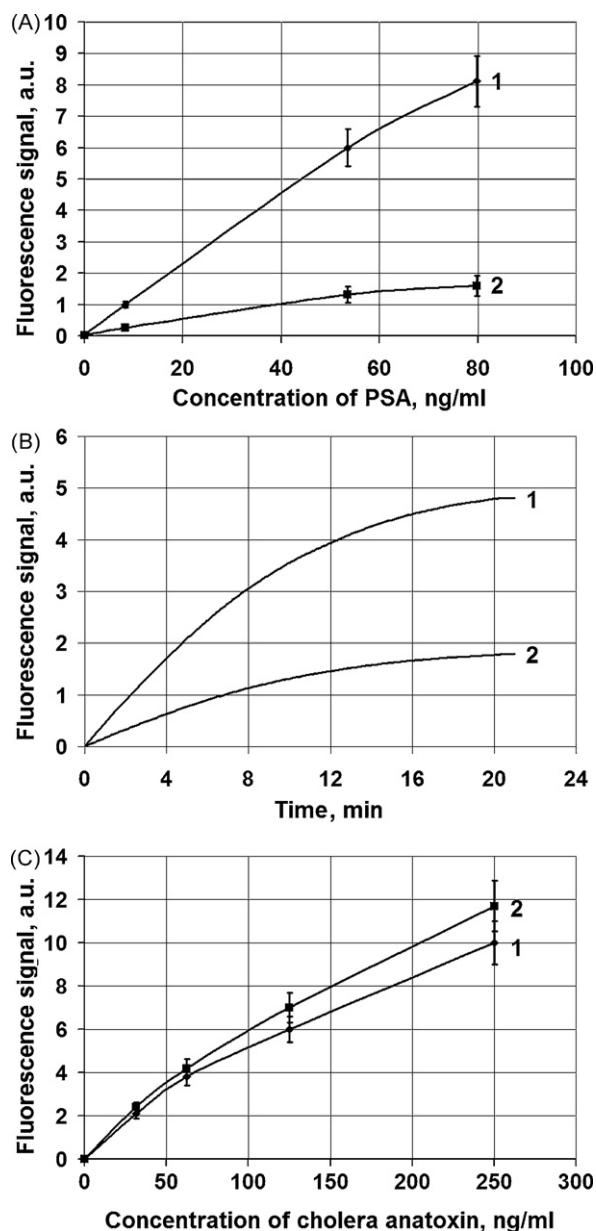


Fig. 7. Calibration curves for immunoassays on plain and metal-coated microchips. (A) Calibration curves for sandwich immunoassay of PSA with protein microchips on metal-coated (1) and glass (2) substrates. In both cases the incubation time was 20 h. (B) Kinetic curves for direct PSA analysis with protein microchips on metal-coated (1) and glass (2) substrates. Concentration of labeled antigen in solution was 80 ng/ml. (C) Calibration curves for sandwich immunoassay of cholera anatoxin with protein microchips on metal-coated (1) and glass (2) substrates. For the microchips on glass substrates the incubation time for binding of immobilized antibodies with antigen and with conjugate of biotinylated antibodies was 17 h, whereas for the microchips on metal-coated substrates it was shortened to 2 h.

of electro-magnetic eigenmodes in dielectric hemisphere on metal surface may be rather complicated (Prokopenko et al., 2006). We tried to interpret the observable features in terms of geometric optics (Fig. 8). Evidently, high reflectivity of metal surface enhances the intensity of excitation radiation of a fluorophore (about twice for perfect reflection; see Fig. 8A). The additional reflection of emitted fluorescent radiation from metal surface may also result in about 2-fold increase of the registered signals (Fig. 8B). Together, this could provide 4-fold enhancement observed for the gel pads with flattened geometry.

The effects of internal reflectance at the boundary of gel pad and emission of radiation from a pad may explain the dependence of

metal-enhanced fluorescence on the shape of the pad and the influence of the liquid covering the pads. In the latter case, the reflection from the external boundary of liquid should also be taken into account (Fig. 8C and D). At the relative refraction index of the gel $n_{gel} \approx 1.4$, about half of fluorescence radiated within the flat layer of gel would be reflected backward and lost through transparent uncoated substrate or reflected from the surface of metal-coated substrates and scattered to the lateral ends of the flat gel after multiple reflections (Fig. 8B).

The photons from a fluorophore molecule near the center of the hemisphere go freely through the boundary of the gel pad (Fig. 8C). The emission from a fluorophore near the boundary would be similar to that from flat layer of gel (cf. Fig. 8B). Such a pattern of emission from hemispherical gel pad may explain the observable ~1.5-fold increase of signals for the hemispherical gel pads on uncoated glass substrates compared with corresponding flattened pads. The radiation reflected backward from the boundary of hemispherical gel pad corresponds to the so-called “whispering gallery” modes (the rays for these modes are shown schematically for the fluorophore nearby gel pad boundary in Fig. 8C) modes. The additional 1.5–2.0-fold factor for fluorescence enhancement in hemispherical gel elements on metal-coated substrate as compared with corresponding enhancement in flattened elements (Fig. 2B) can be explained by the radiation of “whispering gallery” modes. From the optical point of view, a hemispherical gel pad on metal-coated substrate corresponds to a dielectric hemispherical resonator on a conducting surface. The “whispering gallery” modes may finally be emitted from such a resonator (Prokopenko et al., 2006). This fraction of radiation would be lost from gel pads on transparent substrate. The resulting enhancement of fluorescence in hydrated hemispherical gel pads on metal-coated substrate attained 8–10-fold level as compared with the similar pads on transparent substrate.

The emission of fluorescence from the layer of gel and from the layer of liquid covering gel pads should be similar because of low refraction index at the gel–liquid interface (Fig. 8B and D). This means that the enhancement of fluorescence for hemispherical gel pads under a layer of liquid cannot exceed that for the flattened gel pads in the absence of liquid, i.e. ~4. Additional optical losses at the gel–liquid boundary and less efficient excitation of fluorescence in hemispherical gel pads submerged in liquid may explain further suppression of enhancement to ~2.5–3.0-fold for gel pads under liquid in comparison with ~4–5-fold enhancement for flattened pads.

The enhancement of fluorescence by metal coating for hydrated hemispherical gel pads is comparable to the enhancement reported previously for surface microchips (Aslan et al., 2005; Lakowicz, 2005; Sabanayagam and Lakowicz, 2007; Sauer et al., 2005; Strohsahl et al., 2007). As was proved earlier (Zubtsov et al., 2007), the higher immobilization capacity of gel pads results in fluorescence signals an order of magnitude higher than the signals from the surface microchips. This advantage of gel-based microchips remains valid for metal-enhanced fluorescence as well. Therefore, despite the similar extent of fluorescence enhancement on microchips of both types, the difference in the level of signals remains the same.

In the pioneering experiments on the metal-enhanced fluorescence a fluorophore was placed within wavelength-scale distance (~500 nm) from a reflecting metallic surface (reviewed in Sabanayagam and Lakowicz, 2007). Later, experiments on surface microchips proved that the effect persists at much shorter distances of about ~10 nm (Aslan et al., 2005; Lakowicz, 2005; Sabanayagam and Lakowicz, 2007; Sauer et al., 2005; Strohsahl et al., 2007). In our study, the effect of enhancement of fluorescence by metal surface was observed for much longer characteristic distances of up to ~50 μm . Despite the similar level of enhancement, the physical

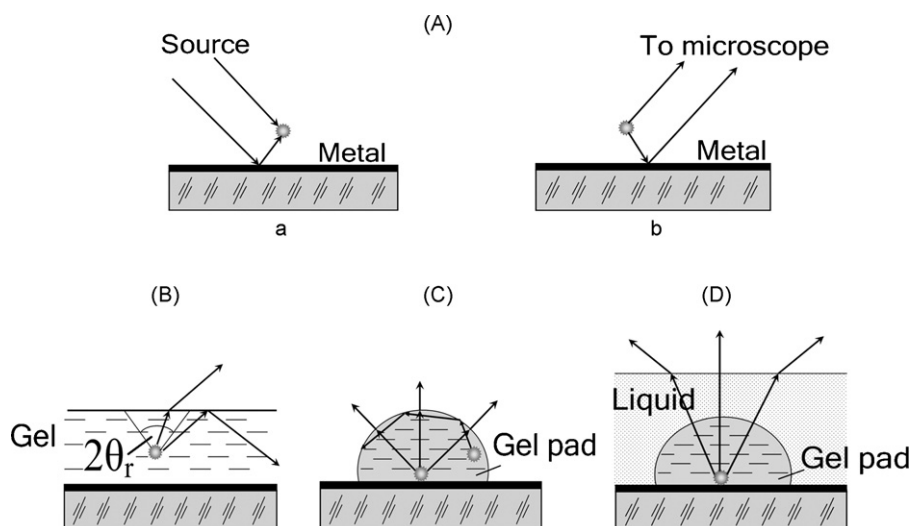


Fig. 8. Geometric optics effects responsible for metal-enhanced fluorescence on gel-based microchips. (A) The reflection of excitation from metal surface provides 2-fold increase in the amount of light reaching the fluorophore (a). Fluorescence microscope registers both direct and reflected radiation emitted by the fluorophore (b). Theoretically, the combination of both effects results in 4-fold enhancement of fluorescence. (B) The emission of radiation from a fluorophore within a flat layer of gel. Rays with incidence angles $\theta < \theta_r$ ($\sin \theta_r = 1/n_{gel}$, where n_{gel} is the refraction index for a gel) go through the upper interface of the gel layer and are registered by fluorescence microscope, whereas rays with incidence angles $\theta > \theta_r$ are reflected backward and lost through transparent uncoated substrate or scattered to the lateral ends of the gel on metal-coated substrates. For $n_{gel} \approx 1.4$ and $\theta_r \approx 45^\circ$ about half of fluorescence radiated within the gel would be reflected backward. (C) The emission of radiation from a fluorophore within hemispherical gel pad. The hemispherical gel pad provides additional enhancement as compared with the flat layer of gel; this enhancement may be more than 2-fold. (D) The emission of radiation from a fluorophore within hemispherical gel pad covered with liquid. The propagation of rays through the upper boundary of the liquid is similar to their propagation through the flat gel interface (see subpart B). Optical losses at the boundary gel–liquid and less efficient excitation of fluorescence within the gel pad under liquid lead to lower fluorescence enhancement for a gel pad covered with liquid as compared with dry flattened gel pads in the absence of liquid.

mechanisms behind the enhancement effects turn out to be different for gel and surface microchips. In particular, the mechanism of fluorescence enhancement for hydrogel-based microchips on metal-coated substrates may be explained within the framework of geometric optics.

5. Conclusion

Metal-enhanced fluorescence is a rapidly developing technology promising significant improvements in fluorescence-based technologies. Our experiments proved that this technique could be successfully applied to gel-based microchips. The enhancement of fluorescence attained ~8–10-fold on microchips with hydrated gel pads and ~4–5-fold on microchips with partially dried gel pads. The use of metal coating allows increasing signal-to-background ratio and therefore sensitivity of immunoassays at the same incubation times or shortening time of analysis without losing sensitivity. As the enhancement of fluorescence on metal-coated substrates is of physical nature, i.e. does not depend on molecular interactions, it can be applied to the analysis of various chemical complexes (DNA, proteins, sugars, etc.) on microchips. Thus, the enhancement of fluorescence by metal coating is a promising direction in further development of microchip technologies.

Acknowledgments

The authors are grateful to S.V. Pan'kov and E.Ya. Kreidlin for their help in microchip fabrication, to A.D. Zalessky for help with confocal microscopy, to D.V. Prokopenko for assistance in preparation of figures, and to I.V. Grechishnikova and S.A. Surzhikov for synthesizing oligonucleotides. Health Front Line, Ltd. (Champaign, IL) assisted in the preparation of this paper. The work was supported by the State Contract no. 02.512.11.2232 from July 07, 2008.

Appendix A.

In this Appendix we discuss briefly the impact of kinetic effects on the sensitivity of immunoassay on gel-based and surface protein microchips. For simplicity, we restrict ourselves to the binary complexes antigen-immobilized antibody. The minimum concentration of antigen defining the sensitivity is determined by the weakest detectable signal depending on the measurement technique and data processing,

$$A[C]_0 = J_{thr} \quad (A1)$$

Here A is the apparatus constant, J_{thr} is the threshold detectable signal, and $[C]_0$ is the concentration of the binary complexes antigen-immobilized antibody within gel pad (or the corresponding surface density in the case of surface microchips) referred to this signal. The concentration of complexes formed for incubation time t_i may be presented as (Kusnezow et al., 2006; Sorokin et al., 2003, 2006),

$$[C]_0 = [C]_{eq} f(t_i/\tau_B; K_a[Ag]) \quad (A2)$$

where K_a is thermodynamic association constant (which is equal to the ratio of association and dissociation rates $K_a = k_{ass}/k_{diss}$), $[Ag]$ denotes the concentration of antigen in solution,

$$[C]_{eq} = [Ab]_{gel} \frac{K_a[Ag]}{1 + K_a[Ag]} \quad (A3)$$

and $[Ab]_{gel}$ is the concentration of immobilized antibodies within gel pad. The function $0 \leq f(t_i/\tau_B; K_a[Ag]) \leq 1$ grows monotonously with incubation time t_i . Its explicit form is rather complicated and is different for the gel-based and surface microchips. In the case of diffusion-limited kinetics the corresponding characteristic times needed for signal saturation are defined by

$$\tau_{B,diff}^{(gel)} \approx \frac{R^2}{D_{gel}} [Ab]_{gel} \frac{K_a}{1 + K_a[Ag]} \quad (A4)$$

$$\tau_{B,diff}^{(surf)} \cong \frac{R}{D_{sol}} [\tilde{A}\tilde{b}_i]_{surf} \frac{K_a}{1 + K_a[Ag]} \quad (A5)$$

where R is the radius of cells, D_{gel} and D_{sol} denote the diffusion coefficients corresponding to the diffusion of antigen in a gel without immobilized antibodies and in analyte solution, and $[\tilde{A}\tilde{b}_i]_{surf}$ corresponds to the numbers of immobilized antibodies per the unit area of surface cell (for the surface microchips). Speeding-up diffusion kinetics by mixing leads to the replacement of R^2/D_{gel} by effective time depending on the mixing conditions (Zubtsov et al., 2006).

The kinetic analysis shows that sensitivity grows with the increase of incubation time. The corresponding dependence is non-linear and multi-parametric. The metal coating does not affect the threshold signal J_{thr} or binding kinetics, but enhances the useful signal related to the formation of complexes (i.e. $A \rightarrow QA$ in Eq. (A1), where Q is the enhancement of signal produced by metal coating). Therefore, the counterpart incubation times at equal sensitivity are related as

$$Qf(t_{i1}/\tau_B; K_a[Ag]) = f(t_{i2}/\tau_B; K_a[Ag]) \quad (A6)$$

Here “1” refers to the microchips on metal-coated substrates, whereas “2” refers to the microchips on glass substrates. Thus, metal coating permits to shorten incubation time at given sensitivity. The simulation of binding kinetics with our program 3D Kinetics for $Q=4$, $\tau_B=10$ h, $t_{i2}=20$ h, and $K_a[Ag]=0.1$ provides about 8.5-fold shortening of incubation time t_{i1} for microchips on metal-coated substrates in accordance with the experimental observations. At the equal incubation times $t_{i1}=t_{i2}$ and the saturated fluorescence signals, the minimum detectable concentration of antigen decreases Q times for the microchips on metal-coated substrates, also in accordance with the results for PSA immunoassay.

References

- Angenendt, P., 2005. Progress in protein and antibody microarray technology. *Drug Discov. Today* 10, 503–511.
- Aslan, K., Gryczynski, I., Malicka, J., Matveeva, E., Lakowicz, J.R., Geddes, C.D., 2005. Metal-enhanced fluorescence: an emerging tool in biotechnology. *Curr. Opin. Biotechnol.* 16, 55–62.
- Barsky, V., Perov, A., Tokalov, S., Chudinov, A., Kreindlin, E., Sharonov, A., Kotova, E., Mirzabekov, A.D., 2002. Fluorescence data analysis on gel-based biochips. *J. Biomol. Screen.* 7, 247–257.
- Born, M., Wolf, E., 1980. *Principles of Optics: Electromagnetic Theory of Propagation, Interference and Diffraction of Light*. Pergamon Press, New York.
- Chechetkin, V.R., Prokopenko, D.V., Makarov, A.A., Zasedatelev, A.S., 2006. Biochips for medical diagnostics. *Russ. Nanotechnol.* 1, 13–27.
- Chen, C.S., Zhu, H., 2006. Protein microarrays. *BioTechniques* 40, 423–429.
- Davis, C., 2005. Introduction to immunoassay principles. In: Wild, D. (Ed.), *The Immunoassay Handbook*. Elsevier, London, pp. 16–31.
- Ford, G.W., Weber, W.H., 1984. Electromagnetic interactions of molecules with metal surfaces. *Phys. Rep.* 113 (4), 195–287.
- Konovalova, E.V., Savvateeva, E.N., Dementieva, E.I., Filippova, M.A., Turygin, A.Yu., Osipova, T.V., Ryabykh, T.P., Rubina, A.Yu., Zasedatelev, A.S., 2007. Development of a biochip with an internal calibration curve for quantitating two forms of the prostate-specific antigen. *Mol. Biol.* 41, 665–669.
- Kusnezow, W., Syagailo, Y.V., Ruffer, S., Klenin, K., Sebald, W., Hoheisel, J.D., Gauer, C., Goychuk, I., 2006. Kinetics of antigen binding to antibody microspots: strong limitation by mass transport to the surface. *Proteomics* 6, 794–803.
- Lakowicz, J.R., 2005. Radiative decay engineering 5: metal-enhanced fluorescence and plasmon emission. *Anal. Biochem.* 337, 171–194.
- Mirzabekov, A.D., Rubina, A.Yu., Pan'kov, S.V., 2003. Composition for polymerizing immobilization of biological molecules and method for producing said composition. Patent of Russian Federation N 2216547, Bull. Izobr. N 32 (in Russian). Patent PCT/RU 01/00420, Patent WO 03/033539.
- Pollack, J.R., 2007. A perspective on DNA microarrays in pathology research and practice. *Am. J. Pathol.* 171, 375–385.
- Prokopenko, Yu.V., Filipov, Yu.F., Shipilova, I.A., Yakovenko, V.M., 2006. Whispering gallery modes in a hemispherical isotropic dielectric resonator with a perfectly conducting planar surface. *Tech. Phys.* 51, 248–257.
- Rubina, A.Yu., Dementieva, E.I., Stomakhin, A.A., Darii, E.L., Pan'kov, S.V., Barsky, V.E., Ivanov, S.M., Konovalova, E.V., Mirzabekov, A.D., 2003. Hydrogel-based protein microchips: manufacturing, properties, and applications. *BioTechniques* 34, 1008–1022.
- Rubina, A.Yu., Pan'kov, S.V., Dementieva, E.I., Pen'kov, D.N., Butygin, A.V., Vasiliskov, V.A., Chudinov, A.V., Mikheikin, A.L., Mikhailovich, V.M., Mirzabekov, A.D., 2004. Hydrogel drop microchips with immobilized DNA: properties and methods for large-scale production. *Anal. Biochem.* 325, 92–106.
- Rubina, A.Yu., Dyukova, V.I., Dementieva, E.I., Stomakhin, A.A., Nesmeyanov, V.A., Grishin, E.V., Zasedatelev, A.S., 2005. Quantitative immunoassay of biotoxins on hydrogel-based protein microchips. *Anal. Biochem.* 340, 317–329.
- Rubina, A.Yu., Kolchinsky, A., Makarov, A.A., Zasedatelev, A.S., 2008. Why 3-D? Gel-based microarrays in proteomics. *Proteomics* 8, 817–831.
- Sabanayagam, C.R., Lakowicz, J.R., 2007. Increasing the sensitivity of DNA microarrays by metal-enhanced fluorescence using surface-bound silver nanoparticles. *Nucleic Acids Res.* 35, e13.
- Sorokin, N.V., Chechetkin, V.R., Livshits, M.A., Vasiliskov, V.A., Turygin, A.Y., Mirzabekov, A.D., 2003. Kinetics of hybridization on the oligonucleotide microchips with gel pads. *J. Biomol. Struct. Dyn.* 21, 279–288.
- Sorokin, N.V., Chechetkin, V.R., Pan'kov, S.V., Somova, O.G., Livshits, M.A., Donnikov, M.Y., Turygin, A.Y., Zasedatelev, A.S., 2006. Kinetics of hybridization on surface oligonucleotide microchips: theory, experiment, and comparison with hybridization on gel-based microchips. *J. Biomol. Struct. Dyn.* 24, 57–66.
- Sauer, U., Preininger, C., Krumpel, G., Stelzer, N., Kern, W., 2005. Signal enhancement of protein chips. *Sens. Actuators B* 107, 178–183.
- Stoughton, R.B., 2005. Applications of DNA microarrays in biology. *Annu. Rev. Biochem.* 74, 53–82.
- Strohsahl, C.M., Miller, B.L., Krauss, T.D., 2007. Preparation and use of metal surface-immobilized DNA hairpins for the detection of oligonucleotides. *Nat. Protoc.* 2, 2105–2110.
- Weaver, J.H., Krafka, C., Lynch, D.W., Koch, E.E., 1981. *Optical Properties of Metals (OPM)*. Physics Data, Nr. 18-1 and 18-2, vols. I and II. Fachinformationzentrum, Karlsruhe, Germany.
- Zubtsov, D.A., Ivanov, S.M., Rubina, A.Yu., Dementieva, E.I., Chechetkin, V.R., Zasedatelev, A.S., 2006. Effect of mixing on reaction-diffusion kinetics for protein hydrogel-based microchips. *J. Biotechnol.* 122, 16–27.
- Zubtsov, D.A., Savvateeva, E.N., Rubina, A.Yu., Pan'kov, S.V., Konovalova, E.V., Moiseeva, O.V., Chechetkin, V.R., Zasedatelev, A.S., 2007. Comparison of surface and hydrogel-based protein microchips. *Anal. Biochem.* 368, 205–213.